

# UK–SOLAS FIELD MEASUREMENTS OF AIR–SEA EXCHANGE

## Instrumentation

BY IAN M. BROOKS, MARGARET J. YELLAND, ROBERT C. UPSTILL-GODDARD, PHILIP D. NIGHTINGALE, STEVE ARCHER, ERIC D'ASARO, RACHAEL BEALE, CORY BEATTY, BYRON BLOMQUIST, A. ANTHONY BLOOM, BARBARA J. BROOKS, JOHN CLUDERAY, DAVID COLES, JOHN DACEY, MICHAEL DEGRANDPRE, JO DIXON, WILLIAM M. DRENNAN, JOSEPH GABRIELE, LAURA GOLDSOON, NICK HARDMAN-MOUNTFORD, MARTIN K. HILL, MATT HORN, PING-CHANG HSUEH, BARRY HUEBERT, GERRIT DE LEEUW, TIMOTHY G. LEIGHTON, MALCOLM LIDDICOAT, JUSTIN J. N. LINGARD, CRAIG MCNEIL, JAMES B. MCQUAID, BEN I. MOAT, GERALD MOORE, CRAIG NEILL, SARAH J. NORRIS, SIMON O'DOHERTY, ROBIN W. PASCAL, JOHN PRYTHERCH, MIKE REBOZO, ERIK SAHLEE, MATT SALTER, UTE SCHUSTER, INGUNN SKJELVAN, HANS SLAGTER, MICHAEL H. SMITH, PAUL D. SMITH, MERIC SROKOSZ, JOHN A. STEPHENS, PETER K. TAYLOR, MACIEJ TELSZEWSKI, ROISIN WALSH, BRIAN WARD, DAVID K. WOOLF, DICKON YOUNG, AND HENK ZEMMELINK

This document is a supplement to “Physical Exchanges at the Air–Sea Interface: UK–SOLAS Field Measurements,” by Ian M. Brooks, Margaret J. Yelland, Robert C. Upstill-Goddard, Philip D. Nightingale, Steve Archer, Eric d’Asaro, Rachael Beale, Cory Beatty, Byron Blomquist, A. Anthony Bloom, Barbara J. Brooks, John Cluderay, David Coles, John Dacey, Michael DeGrandpre, Jo Dixon, William M. Drennan, Joseph Gabriele, Laura Goldson, Nick Hardman-Mountford, Martin K. Hill, Matt Horn, Ping-Chang Hsueh, Barry Huebert, Gerrit de Leeuw, Timothy G. Leighton, Malcolm Liddicoat, Justin J. N. Lingard, Craig McNeil, James B. McQuaid, Ben I. Moat, Gerald Moore, Craig Neill, Sarah J. Norris, Simon O’Doherty, Robin W. Pascal, John Prytherch, Mike Rebozo, Erik Sahlee, Matt Salter, Ute Schuster, Ingunn Skjelvan, Hans Slagter, Michael H. Smith, Paul D. Smith, Meric Srokosz, John A. Stephens, Peter K. Taylor, Maciej Telszewski, Roisin Walsh, Brian Ward, David K. Woolf, Dickon Young, and Henk Zimmelink (*Bull. Amer. Meteor. Soc.*, **90**, 629–644) • ©2009 American Meteorological Society • *Corresponding author:* Ian M. Brooks, Institute for Climate and Atmospheric Science, School of Earth and Environment, University of Leeds, Leeds LS2 9JT, United Kingdom • E-mail: i.brooks@see.leeds.ac.uk • DOI:10.1175/2008BAMS2578.2

**T**he High Wind Air–Sea Exchanges (HiWASE) study, Deep Ocean Gas Exchange Experiment (DOGEE), and Sea Spray, Gas Flux and Whitecap (SEASAW) study brought a wide range of instrumentation and measurement techniques to bear on the problem of parameterizing the physical exchange of gases and aerosol at the air–sea interface. Here, we summarize the primary instrumentation and provide some additional details of measurement systems and techniques. Both DOGEE and SEASAW undertook cruises on the RRS *Discovery*

and made use of core instrumentation maintained and operated by the U.K. Natural Environment Research Council’s (NERC) National Marine Facilities (Table 1). Instrumentation specific to each of the projects is listed in Tables 2 (SEASAW), 3 (DOGEE), and 4 (HiWASE).

**AUTOFLUX.** AutoFlux (Yelland et al. 2009) is an autonomous system for making continuous direct measurements of air–sea fluxes and supporting mean meteorological parameters. It is designed

**TABLE 1. RRS *Discovery* core and joint cruise instrumentation.**

Instrument	Measurement	Group/contact
SBWR	ID wave height spectra	Core instrumentation
Vaisala PTB100A e	Atmospheric pressure	Core instrumentation
Vaisala WAA151	Wind speed	Core instrumentation
Vaisala WAV151	Wind direction	Core instrumentation
Vaisala HMP44L	Air temperature	Core instrumentation
Vaisala HMP44L	Humidity	Core instrumentation
Kipp and Zonen pyranometer	Downwelling solar radiation (335–2200 nm)	Core instrumentation
Skye energy sensor	Downwelling photosynthetically active radiation (400–700 nm)	Core instrumentation
Thermosalinograph	Seawater temperature and salinity	Core instrumentation
Ship's navigation system	Position, heading, velocity	Core instrumentation
AutoFlux–Gill sonic anemometer, 2x LI-COR LI-7500, Systron Donner MotionPak	Turbulent winds (at 19 m), temperature, CO <sub>2</sub> /H <sub>2</sub> O, three-axis accelerations and rotation rates	NOCS, Yelland
Nikon Coolpix 8800 digital cameras	Digital whitecap imagery at 30-s intervals	NOCS, Yelland
PML Live pCO <sub>2</sub> autonomous underway system	pCO <sub>2 (air)</sub> , pCO <sub>2 (water)</sub>	PML–CASIX,* Hardman-Mountford
Aanderaa 3835 optode	Dissolved O <sub>2</sub>	PML–Casix, Hardman-Mountford
CTD system: Sea-Bird 9plus underwater unit	—	Core instrumentation
Sea-Bird 3	Water temperature	
Sea-Bird 4	Conductivity	
Digiquartz P sensor	Temperature compensated pressure	
Sea-Bird 43	Dissolved O <sub>2</sub>	
Chelsea Aquatracka (mk3)	Fluorescence	
Chelsea Aquatracka (mk2)	Transmissometer	
WETlans light scattering sensor	Scattered light	
Chelsea PAR** sensors	Up/downwelling irradiance	
RDI Workhorse 300 KHz ADCP	Ocean current profiles (looking up and down)	

\* Plymouth Marine Laboratory–Centre for Observation of Air–Sea Interactions and Fluxes.

\*\* Photosynthetically active radiation.

to be flexible, allowing different instrumentation configurations to be used as required. The AutoFlux system installed on RRS *Discovery* operated throughout all the U.K.–Surface Ocean–Lower Atmosphere Study (UK–SOLAS) cruises, including SEASAW and DOGEE. This system consisted of two Gill sonic anemometers (an R3 and an MR3) mounted on the either side of the foremast platform, each collocated with a LI-COR LI-7500 CO<sub>2</sub>/H<sub>2</sub>O gas analyzer. A Systron Donner MotionPak mounted at the base of the starboard anemometer measured the three-axis linear accelerations and angular rotation rates from which the ship motion can be determined (Edson

et al. 1998) to correct the measured turbulent wind components. Additional mean temperature and humidity measurements are made by two wet- and dry-bulb psychrometers.

The AutoFlux installation on the *Polarfront* used a single sonic anemometer but two LI-COR LI-7500 gas analyzers. One Licor sensor is kept shrouded, to provide a reference measurement with no turbulent variations in the H<sub>2</sub>O or CO<sub>2</sub> signals. Any remaining variability results from mechanical distortions of the sampling head or the precession of the internal optical chopper induced by ship motion. Spurious correlations between these mechanically induced signals and

**TABLE 2. SEASAW instrumentation. The principal investigator (PI) was I. M. Brooks.**

Instrument	Measurement	Group/contact
Gill sonic anemometer	Turbulent winds and temperature at 21 m	Leeds, <sup>a</sup> I. M. Brooks
CLASP	Aerosol size spectrum 10 Hz, 0.12–9.25 $\mu\text{m}$	Leeds, I. M. Brooks
LI-COR LI-7500	CO <sub>2</sub> /H <sub>2</sub> O concentration	Leeds, I. M. Brooks
FLOS <sup>b</sup>	O <sub>3</sub> concentration	Leeds, McQuaid
TSI ATOFMS	Aerosol single-particle mass spectra 0.1–0.75 $\mu\text{m}$	Leeds, B. J. Brooks
VACC <sup>c</sup>	Aerosol bulk composition via volatility 0.05–1.5 $\mu\text{m}$	Leeds, B. J. Brooks
PMS PCASP <sup>d</sup>	Aerosol size spectra 0.05–3.5 $\mu\text{m}$	Leeds, B. J. Brooks
PMS FSSP <sup>e</sup>	Aerosol size spectra 0.25–23.5 $\mu\text{m}$	Leeds, B. J. Brooks
PMS OAP <sup>f</sup>	Aerosol size spectra 3.55–157.5 $\mu\text{m}$	Leeds, B. J. Brooks
Grimm dust monitor	Aerosol size spectra 0.15–10 $\mu\text{m}$	Leeds, B. J. Brooks
TSI CPC <sup>g</sup>	Aerosol total number concentration	Leeds, B. J. Brooks
Aethalometer	Black carbon aerosol loading	Leeds, B. J. Brooks
CLASP (buoy)	Aerosol spectra at $\sim$ 1 m, 0.12–9.25 $\mu\text{m}$	Leeds, I. M. Brooks
Bubble camera (buoy)	Subsurface bubble spectra at $-$ 0.4 m 30–1000 $\mu\text{m}$	TNO, de Leeuw
UEA pCO <sub>2</sub> instrument (D313) <sup>h</sup>	Continuous mean CO <sub>2</sub> partial pressure in atmosphere and seawater	UEA, Schuster

<sup>a</sup> University of Leeds.

<sup>b</sup> Fast, lightweight ozone sensor.

<sup>c</sup> Volatile aerosol concentration and composition.

<sup>d</sup> Particle Measuring Systems Passive Cavity Aerosol Spectrometer Probe.

<sup>e</sup> PMS Forward Scattering Spectrometer Probe.

<sup>f</sup> PMS Optical Aerosol Probe.

<sup>g</sup> TSI Condensation Particle Counter.

<sup>h</sup> University of East Anglia.

the measured turbulent winds may result in bias and random noise in the derived fluxes. The “flux” values derived from the shrouded unit are used to determine statistical corrections to the fluxes measured by the open unit (Yelland et al. 2009).

**WAVE MEASUREMENTS.** One-dimensional wave spectra were measured by shipborne wave recorders (SBWRs) (Tucker and Pitt 2001) on both the RRS *Discovery* and the *Polarfront*. The SBWR sensors consist of two pairs of accelerometers and pressure sensors mounted port and starboard on the ship’s hull below the waterline, close to the pitch axis of the ship. Data from the port and starboard instrument pairs are combined to eliminate the effects of ship roll, both in accelerations and pressure, and the accelerometer signal is double integrated with respect to time to generate ship heave. The pressure sensors provide a wave height signal additional to the heave, and the two are combined to calculate an in situ wave height. The wave spectra obtained

from the SBWR provide no directional information, so it is difficult to separate wind-driven waves from swell and impossible to determine the orientation of swell to the wind sea. HiWASE supplemented the existing SBWR system on *Polarfront* with the commercial X-band wave radar WAVEX to obtain 2D wave spectra. Although WAVEX provides good directional information, it does not directly measure the wave heights but infers them from a commercially confidential algorithm. Raw data from the SBWR is saved for a 30-min sample period every 45 minutes; WAVEX saves derived quantities every five minutes, and raw data twice per hour. A comparison of data from the two systems shows that WAVEX has a tendency to overestimate wave heights under light wind conditions where swell dominates the wave field (Yelland et al. 2009). The complementary data from the two wave measurement systems—accurate wave heights from the SBWR and directional spectra from WAVEX—provides a complete description of the sea state.

TABLE 3. DOGEE instrumentation.		
Instrument	Measurement	Group/contact
Automated Shimadzu gas chromatographs with electron capture detection	Continuous underway measurement of SF <sub>6</sub> in seawater to locate and map patch and high precision measurement of SF <sub>6</sub> depth profiles for gas exchange and mixing calculations	PML, Nightingale
GC-FID <sup>a</sup>	Measurement of OVOCs in seawater (D320) <sup>b</sup>	PML, Nightingale
Pacific Gyre International drogued Lagrangian drifter buoys	Position, temperature profiles	PML, Nightingale
Noble gas mass spectrometer	Measurement of 3-helium	LDEO/NUT <sup>c</sup> Upstill-Goddard
Pro-Oceanus Systems Inc GTD <sup>d</sup>	Continuous underway dissolved gas concentration	URI, McNeil <sup>e</sup>
Aanderaa Inc. optode	Continuous underway dissolved O <sub>2</sub> , water temperature	URI, McNeil
SAMI sensor, Pro-Oceanus Systems, Inc. pCO <sub>2</sub> sensor <sup>f</sup>	Continuous underway dissolved CO <sub>2</sub>	URI, McNeil
Winkler titrations	Dissolved O <sub>2</sub> from CTD rosette samples	URI, McNeil
Neutrally buoyant floats with SBE O <sub>2</sub> and GTD sensors <sup>g</sup>	Dissolved O <sub>2</sub> and N <sub>2</sub>	URI, McNeil
Varian 3800 gas chromatograph with pulsed flame photometric detector	Dissolved DMS and DMSP concentration	PML, Archer
Metrohm 757 VA Computrace <sup>h</sup>	Total surfactant activity using AC polarography <sup>i</sup>	Newcastle, Upstill-Goddard
Catamaran microlayer skimmer	Surface microlayer water sample collection for subsequent lab analysis for DIC, DOC, DON, NO <sub>3</sub> /NO <sub>2</sub> , NH <sub>4</sub> , PO <sub>4</sub> , SiO <sub>4</sub> , surfactants, chlorophyll-a, DMS, DMSP, MDSO bacterioplankton, phytoplankton, and viral particles (D320)	NIOZ, Zemmeling <sup>k</sup>
MADS <sup>k</sup>	Atmospheric concentration of OVOCs (D320)	Bristol, Young
UEA pCO <sub>2</sub> instrument	Continuous mean CO <sub>2</sub> partial pressure in atmosphere and seawater (D313)	UEA, Schuster
Spar buoy wave system	ID wave spectra, wave breaking, digital still and video imagery	NOCS, Yelland
Spar buoy bubble system	Acoustic bubble spectra (17–1107 μm), optical bubble spectra (0.1–13 mm), sonar imaging of bubble plumes	ISVR, Southampton, Leighton <sup>l</sup>
ASIS	ID wave spectra, turbulent fluxes of momentum, heat, H <sub>2</sub> O, CO <sub>2</sub> , TKE dissipation rate at –1.5 m, water temperature (D320)	Miami, Drennan
ASIS–SAMI pCO <sub>2</sub> sensor, Aanderaa O <sub>2</sub> sensor <sup>m</sup>	Dissolved CO <sub>2</sub> concentration and dissolved O <sub>2</sub> , both at –1.5, –5 m. (D320)	UMT, DeGrandpre <sup>n</sup>
ASIS–LI-COR PAR sensor, fluorometer	Light intensity (–1.5 m) and chlorophyll-a (–5 m) (D320)	UMT, DeGrandpre
ASIS–gas tension device & SBE19plus	Total dissolved gas, DO + CTD + chlorophyll-a, all at –7 m (D320)	URI, McNeil
APIMS	High-frequency atmospheric DMS concentration (D320)	Hawaii, Huebert <sup>o</sup>
Scintillation counter	Measurement of biological uptake rates of radio-labeled methanol	PML, Nightingale
ASIP <sup>p</sup>	Near-surface ocean turbulence (D320)	ODU, Ward <sup>q</sup>

<sup>a</sup> Gas chromatography with flame ionization detection<sup>b</sup> Oxygenated volatile organic compounds<sup>c</sup> University of Newcastle, Newcastle upon Tyne<sup>d</sup> Gas tension device<sup>e</sup> University of Rhode Island<sup>f</sup> Submersible Autonomous Moored Instrument<sup>g</sup> Sea-Bird Electronics<sup>h</sup> Voltammetry<sup>i</sup> Alternating current<sup>j</sup> Royal Netherlands Institute for Sea Research<sup>k</sup> Modified adsorption/desorption system<sup>l</sup> Institute of Sound and Vibration Research, University of Southampton<sup>m</sup> Air–sea interaction spar<sup>n</sup> University of Montana<sup>o</sup> University of Hawaii at Manoa<sup>p</sup> Air–Sea Interaction Profiler<sup>q</sup> Old Dominion University

**TABLE 4. HiWASE instrumentation.**

Instrument	Measurement	Group/contact
Autoflux–Gill sonic anemometer, 2x LI-COR LI-7500, Systron Donner MotionPak	Turbulent winds (height: 15 m), temperature, CO <sub>2</sub> /H <sub>2</sub> O, three-axis accelerations and rotation rates	NOCS, Yelland
Bridge cameras	Digital whitecap imagery at 5-min intervals	NOCS, Yelland
WAVEX radar	2D directional wave spectra	NOCS, Yelland
Kipp and Zonen CM6B pyranometer	Downwelling solar radiation (335–2200 nm)	NOCS, Yelland
Eppley pyrgeometer	Downwelling IR radiation (3.5–50 μm)	NOCS, Yelland
Tasco IR	IR surface temperature	NOCS, Yelland
Sea-Bird MicroTSG <sup>a</sup>	Sea surface temperature and salinity	NOCS, Yelland
SBWR	ID wave height spectra	DNMI
Mean meteorology	Pressure, temperature, humidity, wind speed and direction, water temperature	DNMI
Ship's navigation system	GPS position, speed, course, and heading	DNMI
Radiosonde	Synoptic atmospheric profiles	DNMI
pCO <sub>2</sub> , an O <sub>2</sub> instrument	Continuous mean CO <sub>2</sub> partial pressure in atmosphere and seawater. O <sub>2</sub> seawater only.	BCCR, Skjelvan <sup>b</sup>
CTD	Conductivity–temperature–depth profiles to 1000 m daily, full depth weekly	BCCR, Skjelvan

<sup>a</sup> Sea-Bird microthermosalinograph.

<sup>b</sup> Bjerknes Centre for Climate Research.

Wave wires on the National Oceanography Centre, Southampton (NOCS) spar buoy provide an independent measurement capable of resolving horizontal scales down to approximately 0.14 m (the separation of the wires) and 3 mm in the vertical. One of the aims of the spar buoy was to identify breaking waves from the wave wire data. To verify the nature of waves passing the spar, wave imagery was captured by a digital video camera and two digital still cameras. The video and one still camera face straight down to record images of the waves as they pass through the wave wires. The second still camera was angled toward the horizon to capture images of waves as they approached the buoy and information on more general wave conditions. The camera software did not allow precise synchronization with the logging system, so to allow precise matching of images with the rest of the data, liquid crystal displays showing logging system time were fixed to the dome so as to appear in the corner of the field of view of each camera. Imagery from the still cameras was captured at the rate of 16 images during a 7-s period, with a pause of 7 s between bursts of images on the downward-looking camera, and 9–10 s for the forward-looking camera.

All the cruises used identical pairs of digital cameras mounted in the bridge to obtain imagery of

whitecaps. For analysis, a portion of the image was selected that excluded interference by the ship on the wave field and removed the effects of increased brightness close to the horizon. Images were rejected if they were contaminated by sun glint or sky reflection. A grayscale threshold was selected using the method of Callaghan and White (2008) and a whitecap fraction was determined for each image (Fig. 1). Because of the limited field of view, it is necessary to average multiple images to obtain a statistically robust estimate of the mean whitecap fraction.

**AEROSOL MEASUREMENTS.** Aerosol flux measurements during the SEASAW cruises relied on a new instrument, the Compact Lightweight Aerosol Spectrometer Probe (CLASP), designed and built at the University of Leeds (Hill et al. 2008). CLASP was designed specifically for use in direct eddy covariance flux measurements of marine aerosol, an application with strict requirements on sensor response. Since particle concentrations are typically low in clean marine environments, CLASP has a large sample volume (50 cm<sup>3</sup> s<sup>-1</sup>) compared with many commercial optical particle counters to improve overall counting statistics. This allows the high sample rate (10 Hz) necessary to capture

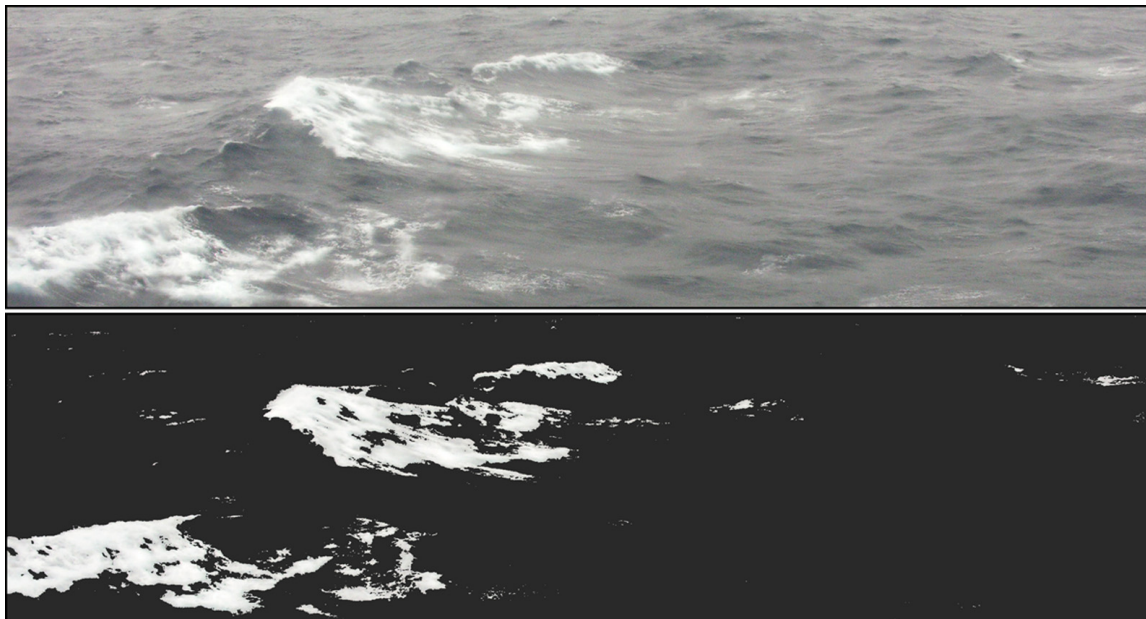


**FIG. 1. (top) Photograph of whitecap from the bridge-mounted camera on *Discovery* taken during D317 on 30 Mar and (bottom) with a mask derived from image processing applied to isolate the whitecaps.**

the full range of turbulence scales. Measuring just  $25 \times 8 \times 6 \text{ cm}^3$ , CLASP can be located very close to a sonic anemometer, eliminating the need for long inlet tubes and the associated problem of particle losses to the walls of the tube.

Background aerosol spectra were measured by a suite of aerosol instruments (see Table 2). Aerosol composition was measured on a single-particle basis by a TSI Aerosol Time of Flight Mass Spectrometer (ATOFMS). Bulk composition and mixing mode were obtained from a volatility system (Brooks et al. 2002), which uses the change in the measured aerosol spectra after heating the sample to infer composition from the characteristic temperatures at which different chemical components become volatile and vaporize. The sample flow is drawn continuously through the system, and the temperature to which it is heated is cycled between ambient and  $900^\circ\text{C}$  every 15 minutes.

**BUBBLE MEASUREMENTS.** The acoustic bubble measurements on the NOCS spar buoy used three transducers (two custom-built and one commercial T135 transducer) to transmit a chain of 14 pulses of increasing frequency. The pulse length is 1 ms, the interval between pulses is 20 ms, and a pause of 1 s is allowed between pulse trains. Four D140 hydrophones are used to record the acoustic signal profile; they are also used, without a transmitted pulse train, to record the noise generated by breaking

waves to estimate initial bubble populations from individual breaking events. A B200 hydrophone was situated on the same plate as the transmit transducers to measure surface reflections and derive a profile of the sea surface.

The bubble imaging system used during SEASAW used a video camera and magnifying optics to image bubbles passing through an illuminated sample volume. The video frames were digitized and saved in 5-s bursts (100 frames), which are saved to disk and the process is repeated. This sequence operates for two minutes out of every five. Image processing software isolates individual bubble from every frame and sizes them to produce mean spectra in the size range from 30 to  $1000 \mu\text{m}$  (in diameter).

**DMS MEASUREMENTS.** The atmospheric pressure ionization mass spectrometer (APIMS) used to make eddy covariance measurements of the turbulent DMS flux was calibrated continuously, measuring both atmospheric dimethyl sulfide (DMS) and an isotopically labeled internal standard at 20 Hz. For 5 min every 2 h, the atmospheric flow was replaced by zero air to calibrate the instrument zero point.

Underway seawater DMS concentrations were obtained from samples drawn using a manual purge-and-trap approach from a towed inlet at less than 2-m depth. The measurement was based around a Varian 3800 gas chromatograph with a pulse flame photometric detector.

**SURFACE FILM MEASUREMENTS.** Water samples from the surface skimmer were analyzed for dissolved inorganic carbon (DIC), alkalinity, dissolved organic carbon (DOC), dissolved organic nitrogen (DON), nitrate/nitrite ( $\text{NO}_3/\text{NO}_2$ ), ammonium ( $\text{NH}_4$ ), phosphate ( $\text{PO}_4$ ), silicate ( $\text{SiO}_4$ ), surfactants, chlorophyll *a* (Chl. *a*), DMS, dimethylsulphoniopropionate (DMSP), dimethylsulfoxide (DMSO), bacterioplankton, phytoplankton, and viral particles.

The surface skimmer was developed to provide greater control over the sampling of the sea surface microlayer (SML) than that provided by commonly used techniques, such as the manual submersion and withdrawal of screens or glass plates. In these processes, the adhered water is subsequently collected into glass bottles by gravity draining water from screens or by wiping water from the glass plate. Although these techniques are appropriate for the sampling of biota and surfactants (Agogu  et al. 2004), withdrawal speed and grid size will likely affect the sampled volumes, and the microlayer sample is potentially diluted with subsurface water. Moreover, transferring the sample from the screen or plate into a glass bottle is time consuming, and several subsamples are needed to collect volumes that are sufficient for analysis. Gas exchange with the surrounding atmosphere makes the use of glass plates or metal screens potentially unsuitable for the sampling of volatiles at the microlayer.

Pilot studies with a prototype surface skimmer showed that it was possible to sample the SML without significant loss of surfactants or bacteria (Frew et al. 2002; Zemmeling et al. 2005); however, these tests also indicated that there will be some loss of volatiles to the atmosphere. For DOGEE a newly developed skimmer allowed the collection of water samples directly into gas-tight bottles, minimizing such losses. To gain insight into potential biases, an intercomparison was carried out between the different sampling techniques. DMS and  $\text{CO}_2$  (solubility at  $20^\circ\text{C}$  is about 11 and 0.7, respectively) were sampled at wind speeds of 15, 10, 5, 1, and 0  $\text{m s}^{-1}$ ; in addition, SF6 (solubility at  $20^\circ\text{C} < 0.01$ ) was sampled at a wind speed of 15  $\text{m s}^{-1}$ . A 7-nM solution of DMS, a 420- $\mu\text{atm}$  solution of  $\text{CO}_2$ , and a 22-pM solution of SF6 were prepared in a 300-L tank. The seawater was thoroughly mixed by a rotating propeller. The surface was sampled by the skimmer, metal screen, and glass plate as described above. A second sample was collected from 0.03-m depth through a stainless steel tube 0.5-cm from the cylinder. By creating the mixed flow and taking water from approximately the same location in the tank, it was assumed that any

difference between the microlayer sample and bulk water sample could be attributed to exchange with the atmosphere—hence, a sampler-related artifact. We have only used the skimmer for the sampling of  $\text{CO}_2$  because of the large volumes (250 mL) needed for the analysis of this compound.

Results show that the loss of DMS from the Garret screen and glass plate is significant: from  $-30\%$  ( $\pm 11\%$ ,  $n = 9$ ) at 0  $\text{m s}^{-1}$  increasing to  $70\%$  ( $\pm 9\%$ ,  $n = 9$ ) at wind speeds of 15  $\text{m s}^{-1}$ . Although we only sampled SF6 at a wind speed of 15  $\text{m s}^{-1}$ , results show that the manual sampling systems introduce a loss of nearly 90% ( $\pm 3\%$ ,  $n = 5$ ). The loss of SF6 from the skimmer at a 15  $\text{m s}^{-1}$  wind speed is 35% ( $\pm 2\%$ ,  $n = 5$ ), comparable to the 30% ( $\pm 15\%$ ,  $n = 9$ ) loss of the more soluble gas DMS. The skimmer introduces a small DMS loss of 2% ( $\pm 6\%$ ,  $n = 9$ ) to 6% ( $\pm 5\%$ ,  $n = 9$ ) at 0 and 5  $\text{m s}^{-1}$  wind speed, respectively. The DMS loss increases to 20% ( $\pm 5\%$ ,  $n = 9$ ) at a wind speed of 10  $\text{m s}^{-1}$ . Carbon dioxide, a gas with an intermediate solubility, was sampled in a laboratory with atmospheric  $\text{CO}_2$  values of 1100  $\mu\text{atm}$ . Microlayer concentrations show a profound increase from 22% ( $\pm 5\%$ ,  $n = 10$ ) to 40% ( $\pm 10\%$ ,  $n = 10$ ) at wind speeds of 10 and 15  $\text{m s}^{-1}$ , respectively. The increase is less profound at lower wind speeds, where  $\text{CO}_2$  increased 2% ( $\pm 3\%$ ,  $n = 10$ ) at 0  $\text{m s}^{-1}$  and 9% ( $\pm 6\%$ ,  $n = 10$ ) at 5  $\text{m s}^{-1}$ .

From these tests, we conclude that the Garret screen and the glass plate cannot be used for sampling volatiles in the microlayer. At low wind speeds, loss factors from the skimmer are relatively small, at least within the systematic precision of our analytical instruments. At 5  $\text{m s}^{-1}$  the sampling error starts to increase and care has to be taken when using the skimmer for sampling volatiles in the microlayer above this wind speed.

## REFERENCES

- Agogu , H., and Coauthors, 2004: Comparison of samplers for the biological characterization of the sea surface microlayer. *Limnol. Oceanogr.: Methods*, **2**, 213–225.
- Brooks, B. J., M. H. Smith, M. K. Hill, and C. D. O’Dowd, 2002: Size-differentiated volatility analysis of internally-mixed laboratory-generated aerosol. *J. Aerosol Sci.*, **33**, 555–579.
- Callaghan, A. H., and M. White, 2009: Automated processing of sea surface images for the determination of whitecap coverage. *J. Atmos. Oceanic Technol.*, **26**, 383–394.
- Edson, J. B., A. A. Hinton, K. E. Prada, J. E. Hare, and C. W. Fairall, 1998: Direct covariance flux estimates

- from mobile platforms at sea. *J. Atmos. Oceanic Technol.*, **15**, 547–562.
- Frew, M. F., R. K. Nelson, W. R. McGillis, J. B. Edson, E. J. Bock, and T. Hara, 2002: Spatial variations in surface microlayer surfactants and their role in modulating air–sea exchange. *Gas Transfer at Water Surfaces, Geophys. Monogr.*, Vol. 127, Amer. Geophys. Union, 153–159.
- Hardman-Mountford, N. J., and Coauthors, 2008: An operational monitoring system to provide indicators of CO<sub>2</sub>-related variables in the ocean. *ICES J. Mar. Sci.*, **65**, 1498–1503, doi:10.1093/icesjms/fsn110.
- Hill, M. K., B. J. Brooks, S. J. Norris, M. H. Smith, I. M. Brooks, and G. de Leeuw, 2008: A Compact Lightweight Aerosol Spectrometer Probe (CLASP). *J. Atmos. Oceanic Technol.*, **25**, 1996–2006.
- Pierrot, P. D., and Coauthors, 2008: Recommendations for autonomous underway pCO<sub>2</sub> measuring systems and data reduction routines. *Deep Sea Res. II*, doi:10.1016/j.dsr2.2008.12.005.
- Tucker, M. J., and E. G. Pitt, 2001: *Waves in Ocean Engineering*. Ocean Engineering Book Series, Vol. 5, Elsevier, 521 pp.
- Yelland, M. J., R. W. Pascal, P. K. Taylor, and B. I. Moat, 2009: AutoFlux: An autonomous system for the direct measurement of the air–sea fluxes of CO<sub>2</sub>, heat and momentum. *J. Oper. Oceanogr.*, **2** (1).
- Zemmelink, H. J., L. Houghton, N. M. Frew, and J. W. H. Dacey, 2005: Gradients in dimethylsulfide, dimethylsulfoniopropionate, dimethylsulfoxide, and bacteria near the sea surface. *Mar. Ecol. Prog. Ser.*, **295**, 33–42.